



ELSEVIER

Contents lists available at ScienceDirect

Opto-Electronics Review

journal homepage: <http://www.journals.elsevier.com/opto-electronics-review>

Photo-reception properties of common LEDs

M. Kowalczyk*, J. Siuzdak

Institute of Telecommunications, Warsaw University of Technology, 15/19 Nowowiejska Str., 00-665, Warsaw, Poland

ARTICLE INFO

Article history:

Received 18 January 2017

Received in revised form 3 May 2017

Accepted 16 June 2017

Available online 24 July 2017

Keywords:

LEDs as photo-detectors

Visible light communication (VLC)

Bi-directional transmission

ABSTRACT

The article proves that common LEDs may act as photodetectors with limited sensitivity, if they are polarized with an appropriate reverse voltage. The measured responsivities are ranged between 0.002 and 0.156 A/W and they depend on the LED type. The only one exception are white (phosphorescent) LEDs which do not exhibit any photosensitivity. There have also shown that a bandwidth of LEDs, which were examined in a role of photodetectors, is of a few tens of MHz, which is an order of magnitude greater than their modulation bandwidth as transmitters. The reasons of the observed LEDs behaviour are explained theoretically. The obtained results are indicated that some of them may be used as both transmitters and receivers in the VLC links working in a bi-directional half-duplex mode.

© 2017 Association of Polish Electrical Engineers (SEP). Published by Elsevier B.V. All rights reserved.

1. Introduction

Currently, the light emitting diodes (LEDs) are widely used as light sources for lighting purpose, as well as transmitters in various communications systems in a visible and infrared scope. It is also known, for some time, that unbiased (a photovoltaic regime) or reversely polarized LEDs can act as photo-detectors [1,2]. There are some attempts to employ this property in a process of construction of various experimental devices and systems. As an example, we can mention here the communication applications like half-duplex plastic optical fiber systems using LEDs in a double role both as transmitters and photo-receivers [3], as well as wireless optical networks operating according the same principle [4–11]. Among other applications are material science [12,13], different kind sensors [14–16], remote sensing [17–19], as well as photometry [2,20]. A quite large number of applications in which the LEDs are or may be used in a role as photodetectors is not surprise, if we take into account their commonness, reliability and low cost. Furthermore, it is expected that the development of the optical wireless transmission systems, acting in a visible light range should contribute to the further popularization of this approach, especially, if it is known that such transmission with data rate more than 100 Mbps is possible in regard to the systems of this type, in which the LEDs are used both for transmitting, as well as receiving, it has been confirmed experimentally recently [4,5]. Unfortunately, what is known about LEDs acting as photodetectors is rather limited and may be summarized as follows. The LEDs can act as the

wavelength-selective photodetectors for wavelengths shorter than they emit in a range difference between wavelengths on which they are sensitive not exceeding 100 nm [1,2,12]. An increase of applied reverse voltage diminishes the junction capacitance and boosts the operation speed [1,12]. The widths of the impulse response of the order of a few nano seconds were measured with the use of high reverse voltage [1,21]. Simultaneously, the high reverse bias leads to the avalanche multiplication effect of the carriers and increases the photo-current. Multiplication factors as high as 20 were measured [12]. However, the mentioned results were obtained for few of selected LEDs only. To the best of our knowledge, there is a lack of a work where a greater number of LEDs has been examined in terms of their photo-detection properties and usefulness for the communications' purpose. Moreover, there is no work, which refers to the actual values of the LED photo-detector responsivity, R , in A/W, which is a crucial parameter for many systems, where LEDs acting as photodetectors have a chance to be applied. The only one exception is Ref. [4], which gives the value of $R=0.021$ A/W for an unbiased LED. A lack of such knowledge can be an important constraint in the development of this type systems in future.

The work aims at filling this gap. Among others were measured the absolute values of the responsivity R for a group of several different types of LEDs emitting colours ranging from red to blue as well as for the white LEDs. Furthermore, the measurement of their frequency response as photodetectors have been performed. Also, the reasons behind such LEDs' behaviour are discussed in some details. The obtained results indicate among others that some LEDs may be used as both transmitters and receivers in the half-duplex visible light communications (VLC) systems.

* Corresponding author.

E-mail address: mkowalczyk@tele.pw.edu.pl (M. Kowalczyk).

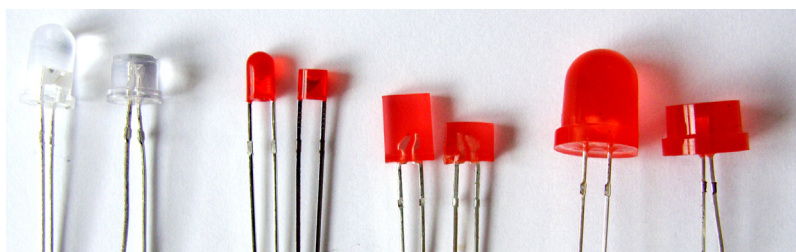


Fig. 1. The examined LEDs before and after lens removing.

Table 1

A size of active areas for the selected types of LEDs.

LED type	Emitted Colour	Manufacturer	S_{LED} [mm ²]
C503B-RAN	Red	CREE	0.44
C503B-AAN	Amber	CREE	0.44
RS 5035PY	Yellow	Dragon	0.34
C503B-GAS	Green	CREE	0.55
C503B-BAS	Blue	CREE	0.55
C503D-WAN	White	CREE	0.45
JZL-RO803D-C0	Red	JIUZHOU OPTOELECTRONICS	0.3
JZL-R6B2D-L0	Red	JIUZHOU OPTOELECTRONICS	0.04
HL-304S42FC	Red	HONGLITRONIC	0.08
FYL-3004SRD1D	Red	FORYARD Optoelectronics	0.22

2. Measurement of led responsivity R

In order to measure an exact value of the responsivity parameter, R , in [A/W] we used LEDs, where their plastic lenses were rubbed off previously, as it has been depicted in Fig. 1. Lens' removing is necessary because it has properties of a light focusing, which means that an incident light power intercepted by the LED with a lens is (much) greater than it would follow from the value of its photo-sensitive area. As a result, a flat surface was obtained, in such way that the remaining polymer layer thickness is minimum but enough to prevent the LED structure from damaging. Having the LEDs prepared in this way, in the next step we measured the value of the LED's active areas.

We assumed that the photo-receiving area is the same as the emitting area since we have no means to distinguish between these two. To the calculation of the active areas' size we used a measuring microscope, where the LED structure was observed while in emission mode. The measurement results have been summarized in Table 1.

It is worth mentioning that shapes of the emitting areas can be quite complicated, as it has been shown in Fig. 2; here, the active area consists of a central square and an encompassing ring.

A measurement of the responsivity parameter was carried out based on a comparative method with use of a setup depicted in Fig. 3. In the first stage, there was measured the surface power density (in W/m²) of the light flux originating from a monochromator at the given wavelength λ and at a given point in space. To this end a reference photodiode was used (VTP 1220FBH), for which the value of the active area, S_p , was taken from its data sheet together with its responsivity characteristics, $R_p(\lambda)$. The values of the photocurrent originating from this photodiode, I_p , were measured for tested wavelengths with a step of 5 nm. In the second stage, the reference photodiode was replaced with the LED under test, which was placed at exactly the same space point, and the values of photocurrent generated by the LED, I_{LED} , were measured as a function of wavelength change. Knowing previously a size of the active area, S_{LED} , of the examined LED at this moment at this stage based on the results from the previous one, we can calculate quite easily the

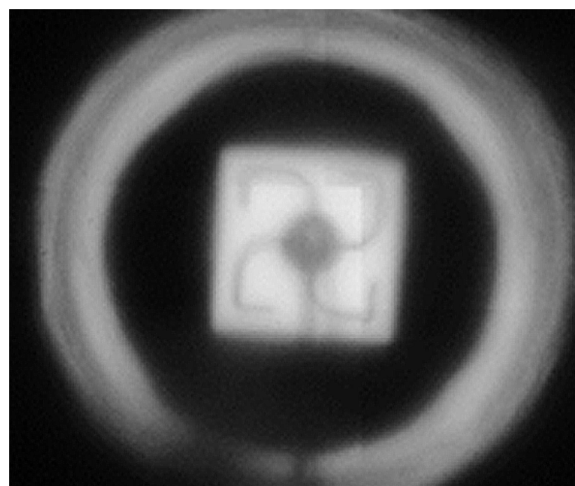


Fig. 2. Photo of the active area of C503B-RAN LED while in emission mode.

value of its responsivity, R , at the λ wavelength, $R_{LED}(\lambda)$, according with Eq. (1).

$$R_{LED}(\lambda) = R_p(\lambda) \frac{S_p}{S_{LED}} \cdot \frac{I_{LED}(\lambda)}{I_p(\lambda)} \quad (1)$$

The obtained responsivity values, $R(\lambda)$, for the various LEDs, for different reverse voltages, U_R , have been shown in Fig. 4.

In the same figure, the photocurrent of a current gain (multiplication factor M) is depicted as a function of the reverse voltage. Here, the photovoltaic current ($U_R = 0$) is used as a reference. In turn, Table 2 lists the maximum values of $R(\lambda)$ denoted by R_{MAX} obtained for various LEDs at different reverse voltages.

It was observed that when the LED chip temperature increased the wavelength of the maximum sensitivity moved towards greater wavelengths but still was below the emission maximum. The results shown in all figures and tables were obtained under thermal equilibrium conditions. Generally, the sensitivity of LED as a photo-detector (its responsivity) increases with the increase of the reverse voltage. However, details about how strong is this relation depend very much on the diode type. The current gain/multiplication factors equal to 2...10 were observed for some LEDs (eg. JZL-RO803D-C0). On the other hand some LEDs are relatively insensitive to the reverse voltage changes (eg. RS-503PY). The measured maximum values of the R are ranged from around 0.002 A/W to 0.156 A/W for monochromatic diodes. However, the white (phosphorescent) LEDs (eg. C503D-WAN) proved to be light insensitive (typically, $R=0$ within the measurement error) most probably due to the high attenuation introduced by the phosphorescent layer. We observed that the increasing reverse voltage apart from the boost of photocurrent also enforces of a certain increase of the wavelength sensitivity range. This effect is particularly visible in case of C503B-RAN LED (Fig. 4). We will discuss the obtained results in the fourth paragraph. It is necessary to stress that apart

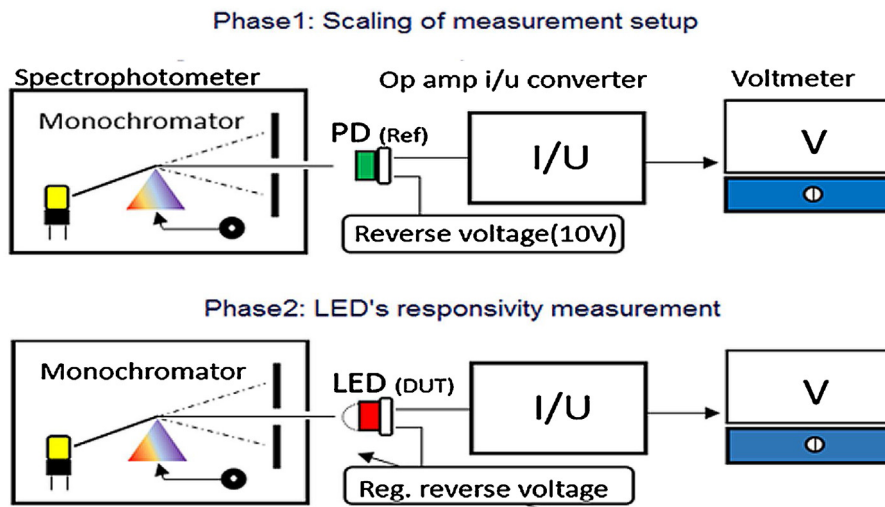


Fig. 3. The measurement way of the values' responsivity parameter, R , in A/W .

Table 2

The maximum values of the responsivity measured for selected reverse voltages of several LED types.

LED type	λ_{peak} nm	U_{R0} V	R_0 A/W	U_{R1} V	R_1 A/W	U_{R2} V	R_2 A/W	U_{R3} V	R_3 A/W
C503B-RAN	595	0	0.077	10	0.083	20	0.086	30	0.1024
C503B-AAN	590	0	0.067	10	0.090	20	0.121	30	0.156
RS 5035PY	565	0	0.070	10	0.078	20	0.080	30	0.082
C503B-GAS	435	0	0.0035	2.5	0.0036	5	0.0037	7.5	0.0039
C503B-BAS	415	0	0.0014	2.5	0.0016	5	0.0018	10.5	0.0028
C503D-WAN	–	–	–	–	–	–	–	–	–
JZL-RO803D-C0	610	0	0.0016	10	0.0061	20	0.011	30	0.015
HL-304S42FC	620	0	0.0048	10	0.0052	20	0.0067	30	0.0095
FYL-3004SRD1D	645	0	0.00006	5	0.00012	10	0.00018	15	0.0022

from the possible difference between the real value of emitting and detecting LED's areas the used measurement approach did not take into account the attenuation of polymer layer remaining after the lens polishing, although we believe it should be very small.

3. Measurement of leds' bandwidth as photodetectors

In order to determine the potential of the LEDs as a receiver in transmission systems there was carried out a measurement of the frequency responses of transmission links, where the LEDs were used in a double role, i.e. as a light source at the transmitter (a normal bias was applied here) and as a photodetector at the receiving node (a reverse bias). The block scheme of the measurement setup has been depicted in Fig. 5.

At the transmitter side as a signal source a sweep generator was used. It is an integral part of a spectrum analyzer (Rohde & Schwartz FSH6). In this way it generates a sine signal with a changing sweep frequency that drove an optical transmitter (LED or a red laser used for comparison). The LEDs used as transmitters were polarized (a nominal point of work) with a DC bias current, which was set at a value typical for a given device (20 mA at the most cases). Obtained in this way an optical signal of the reference was fed to a photodetector (the LED with a reverse bias or a p-i-n photo-diode used for comparison) via a short (4.3 cm) glass fiber of a 5 mm diameter. After the photo-detection the obtained signal was amplified with using a trans-impedance amplifier and, next passed to the spectrum analyzer input, a second integral part of the FSH6 device. The eventual influence of the setup frequency characteristics on final results has been eliminated on a way of the device calibration procedure. The measurements results have been presented in Fig. 6. It

is readily seen that the 3 dB bandwidth of the LED-LED link is limited by the LED transmitter modulation bandwidth, not a bandwidth of the LED receiver. The former is around 5 MHz for each tested LED, whereas the latter varies between 25...65 MHz depending on the LED type and intensification of the reverse polarization.

4. Discussion

Unfortunately for our research, a very little of it has been disclosed by manufacturers with regard to the devices' construction details which were examined. In fact, we did not have any information even about the used materials. Therefore, our further analysis is restricted to be very general and it is based on common knowledge. It is known, that AlGaInP and InGaN are dominant materials which are used in commercially available LEDs for red/amber/yellow, and green/blue colours, respectively [22,23]. Thus, we may safely assume that, if we talk about the LEDs which characteristics were presented in Fig. 4, the first three (i.e. red, amber, and yellow) LEDs are made of AlGaInP, and the last two (i.e. green, and blue) are made of InGaN. This is further confirmed by their forward voltages, which are around 2.1 V@20 mA for the first three LEDs, and around 3.2 V@20 mA for the last two. Since all of them are highly efficient HBLED (>5 cd@20 mA) we presume in the sequel that all of them are based on hetero-structures due to homo-junctions are much worse in this regard [22,23]. Moreover, typical InGaN LEDs are Multiple Quantum Well (MQW) structures. In summary, we assume that the first three LEDs (red, amber, yellow) are Double Hetero-junction (DH) AlGaInP devices (no quantum wells), and the last two are DH MQW InGaN structures. The typical width of active layer of DH AlGaInP device (no QW) is of a few tenths of microm-

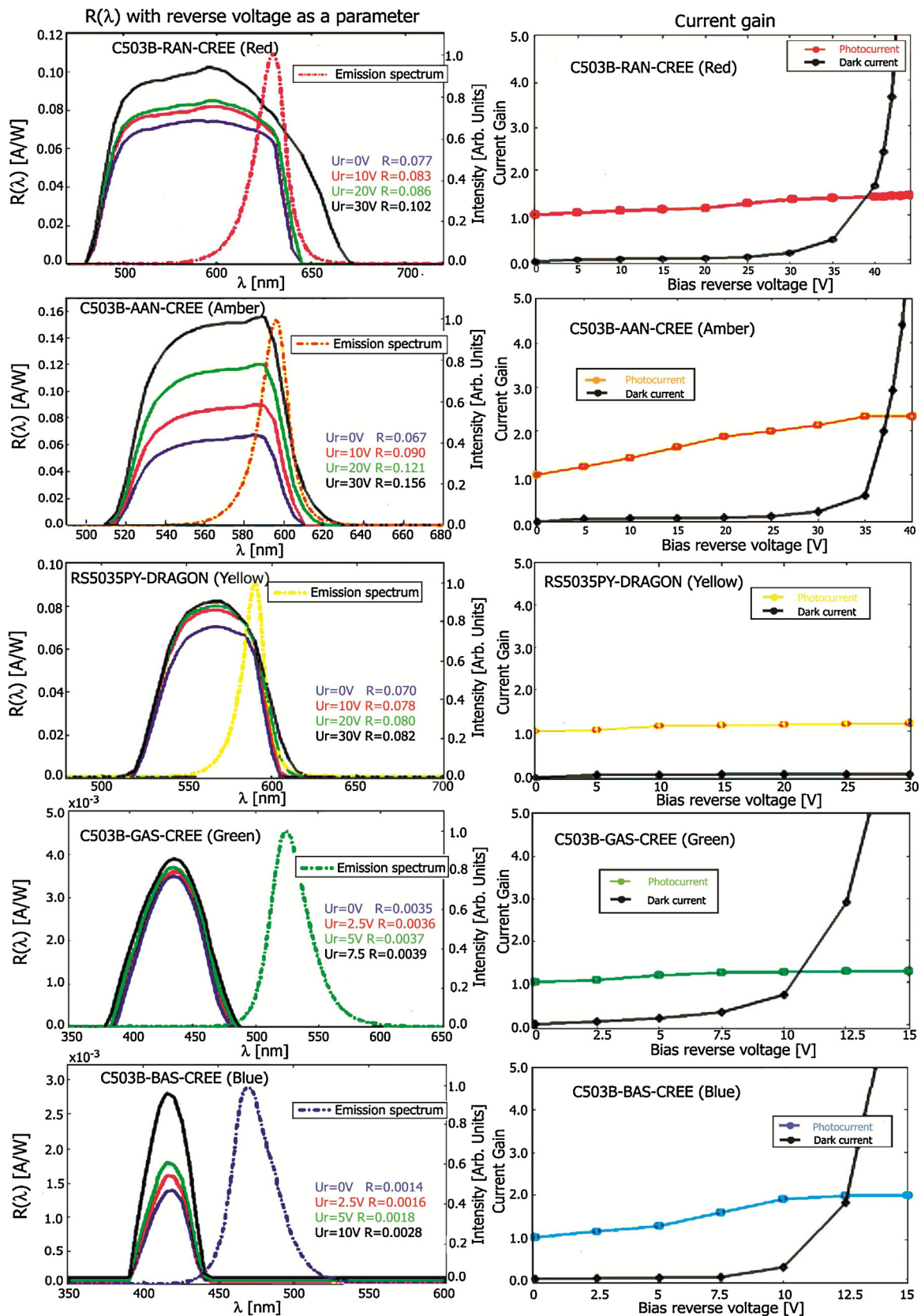


Fig. 4. The responsivity characteristics, $R(\lambda)$, in A/W, in a function of wavelength and the reverse voltage of chosen LEDs and their emission spectrum in arbitrary units, as well as multiplication factor/current gain against the reverse voltage (right side).

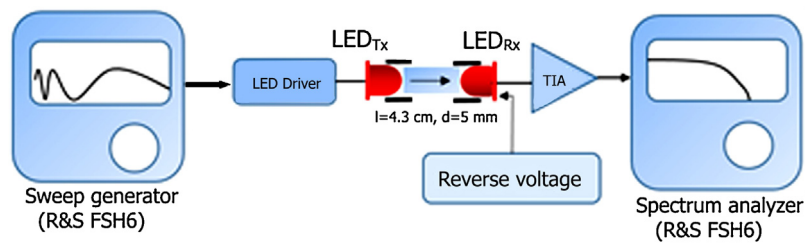


Fig. 5. A block schema of the frequency response measurement setup.

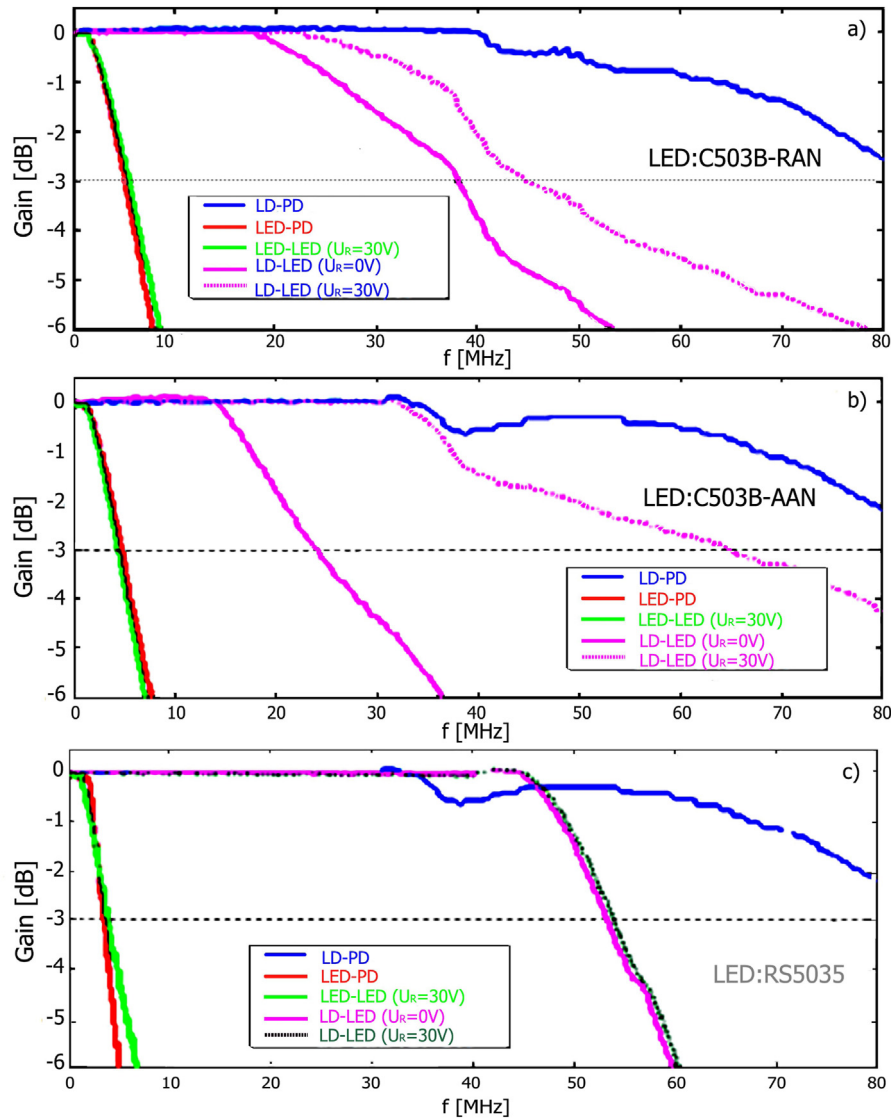


Fig. 6. Frequency characteristics of the LED-LED link measured for different LEDs and different transmitter receiver combinations (LD- laser diode, PD- photo-diode): a) red, b) amber, c) yellow.

eter ($0.15 \dots 0.75 \mu\text{m}$) [22,23], whereas the width of active layer in InGaN MQW DH LED is of order of magnitude lower, i.e. it is a few tens of nanometers [23,24]. Both widths are well within diffusion lengths of minority carriers, which are a few micrometers for AlGaInP [23,25], and a few hundreds of nanometers for InGaN [24,26]. LEDs are deliberately designed so that the active layer width is less than the minority carrier diffusion length because only then the benefits of carrier confinement may be fully realized [27]. A reversely biased LED acts as a poorly designed photodiode where the photocurrent flow is caused by the generation of

electron-hole (EH) pairs in the entire active layer (as the latter is within the minority carrier diffusion length from the junction), and the junction itself. We do not think that the generation of EH pairs may actually take place in the confining layers that surround the active layer because the former have much higher energy band gap. First, let us discuss the variation of the LED responsivity for AlGaInP red/amber/yellow LEDs shown in Fig. 4. In all these figures the LED emission spectrum is depicted for comparison. It may be assumed that the longest emitted wavelength corresponds roughly to the band gap energy of the active layer [22,23]. It means that the

responsivity of LED used as a photodiode should be zero beyond this point (i.e. towards the longer wavelengths). It is agreed very well with our research with one exception, i.e. the highest reverse voltages. We attribute this discrepancy to the Franz-Keldysh effect, i.e. roughly speaking of the reduction of energy band gap when a high reverse bias is applied to the junction. Such effect was observed in materials like GaInP [28]. The short wavelengths cut-off, which is observed in all the responsivity curves is typical for any photodiode and it follows from the rise of absorption coefficient for short wavelengths. However, the spectral sensitivity range is much narrower (70...130 nm for the red/amber/yellow LEDs) than for regular photodiodes (several hundred nanometers). This may be explained as follows. If the photon energy exceeds the band gap of the confining layer it generates EH pair there, which recombines before it reaches the junction and does not contribute to the photocurrent (and responsivity). Now, let's turn to the InGaN green/blue LEDs with characteristics shown in Fig. 4. The most prominent difference is that the responsivity spectral range is completely separated from the emission spectrum. We attribute this behaviour to the QW structure of the active layer. Let us assume that the QW energy band gap is E_1 , whereas the surrounding energy barrier is E_2 ($E_2 > E_1$). The emission spectrum roughly corresponds to E_1 [22,23]. However, if the photon with energy E , $E_2 > E > E_1$ generates EH pair within the QW, the minority carrier (electron in p layer) is trapped in conduction band within QW by the potential barriers and does not contribute to the photocurrent. Only the photons with energies $E > E_2$ may generate minority carriers that are able to reach the junction and give rise to the photocurrent. This explains also the much narrower (30...70 nm) spectral responsivity range of InGaN LEDs used as photodiodes because the emission range is excluded from it. We can also notice that the maximum measured R magnitude for InGaN LEDs (0.002...0.004 A/W) is one-two orders of magnitude less than the respective value (0.07...0.15 A/W) for AlGaInP LEDs. Apart from obvious reasons that the different materials are used, and the R always decreases with the wavelength reduction due to the greater photon energy, we also attribute this difference to the thickness of the InGaN active layer, which is an order of magnitude thinner than in an AlGaInP device, thus limiting the photon collection abilities of the InGaN device. Last but not least we may also observe that the responsivity increases with the rise of the reverse bias intensity. A strength of the effect varies from device to device but the tendency is common. When the reverse voltage (U_R) is increased, the depletion layer widens proportionally to $\sqrt{U_0 + U_R}$, where U_0 is the built-in voltage [22]. Apart from reducing the junction capacitance this widening may increase the volume in the confinement layer, in which the photo-generation of EH pairs takes place. However, it does not change similar volume in the active layer, as the entire span of the latter is well within minority carriers diffusion length. The increase of the reverse voltage slightly improves also the charge collection efficiency. Another effect that may take place when the reverse voltage is increased is the avalanche multiplication within the junction due to the electric field intensity increase. In fact, it is the effect which is referred by the most of authors when they observed this phenomenon [1,12]. The multiplication factor, M, may be approximated as [22]:

$$M = \frac{1}{1 - \left(\frac{U_R}{U_{BT}}\right)^n} \quad (2)$$

Here U_{BT} is a value of the break voltage, and the n value depends on the device [22]. Since the junction width is roughly proportional to the square root of reverse bias, the 10 V increments of the reverse voltage would cause less and less responsivity improvement as U_R rises if the junction width change was the reason. Moreover, the overall improvement is expected to be moderate in this case. Such a behaviour is observed in Fig. 4 only for the yellow LED, which was

produced by a different manufacturer than the rest of the devices. This is confirmed by a lack of the increased dark current in response to rising U_R (see Fig. 4, right column). This rise is probably caused by the quantum tunneling effect, and it is visible for all other LEDs. Moreover, the third LED has a very high break through voltage (>80 V) so the avalanche multiplication effect is rather improbable in this case. Therefore, we assigned its behaviour to the first group of effects. On the contrary, in a case of all the remaining LEDs the increments in their responsivity are greater for higher absolute value of U_R , which well agrees with Eq. (2). Moreover, more than twice the increase in responsivity is observed here for some devices, and even more than that in some publications [1]. This would be difficult to explain based only on the first group of the effects. Therefore, we assumed that the behaviour observed in four remaining LEDs is caused by the avalanche multiplication effect. This is indirectly confirmed by the LEDs data sheets: the higher the admissible reverse voltage, the smaller the gain current for a given reverse bias.

For all examined LEDs we observed the 3 dB modulation bandwidth around 5 MHz when they are used as a light source. On the contrary, if they are used as photodetectors their 3 dB bandwidth varies between 25 and 65 MHz depending on the device and the applied reverse voltage, U_R . In two cases (Fig. 6a, b), the reception bandwidth increased with the U_R absolute magnitude most probably due to the reduction of the junction capacitance, C, with the reverse voltage increase. However, in one instance (device from different manufacturer- Fig. 6c) the reception bandwidth was insensitive to the change of the U_R , most probably because the junction capacitance was small anyway. Since the junction capacitance is inversely proportional to the junction width it may be concluded that this width is the smallest for the amber LED shown in Fig. 6b (the greatest change of bandwidth with U_R), it is intermediate for the red diode of Fig. 6a, and it is the greatest for the yellow LED of Fig. 6c, as in the last case the reverse voltage increase did not cause any visible bandwidth change. This observation well correlates with the LED responsivity, R, dependence on the reverse voltage shown in Fig. 4 (left column). We have attributed this effect to the avalanche multiplication, and now this is confirmed by the bandwidth measurements mentioned above. The avalanche multiplication will be the most pronounced in a LED with a narrow depletion layer (junction) as the electric field has the highest intensity. It is exactly so. The amber diode with the narrowest junction exhibits the greatest increase of R with the U_R , whereas the yellow LED with the widest junction is relatively insensitive to the U_R changes. The red LED with the medium junction width is located somewhere in between. The differences between bandwidths in the emission and reception modes follow from the fact that the LED emission bandwidth is inversely proportional to the effective recombination time [24], whereas the reception bandwidth (neglecting RC constant) is inversely proportional to the transit, and diffusion times [22] that are much shorter than the effective recombination time.

5. Conclusions

The work proves that LEDs may act as photodetectors with limited sensitivity under photovoltaic regime or if they are polarized with an appropriate reverse voltage. The measured responsivities ranged between 0.002 and 0.156 A/W and depended on the LED type. The only one exception are white (phosphorescent) LEDs, which do not exhibit any photosensitivity. We have also shown that a bandwidth of LEDs, which were examined in a role of photodetectors, is a few tens of MHz, which is an order of magnitude greater than their modulation bandwidth as transmitters. As it is already known and it has been confirmed in the paper in regard to

the same LED is a lack of full matching between the peak emission wavelength and the wavelength for which its photosensitivity is the highest. Wherein the maximum of the photosensitivity occurs for the wavelengths shorter than the peak emission wavelengths. However, the ranges of photosensitivity and emission at least partly overlap for some LEDs (see Fig. 4). This indicates that the same LEDs may be used as transmitters and receivers in the half-duplex mode, typically with moderate bitrate, as long as the high reception sensitivities are not required. Generally, the responsivities of high brightness LEDs (HBLED) are comparable with parameters offered by the conventional p-n photodiodes without additional intrinsic layer. What it is also important the concept of using the low-cost LEDs from a shelf in a double role is not only a theoretical vision, but was confirmed fully at the experimental way. The implementations of this type systems as a proof of the concept were reported for the last time among others with reference to Refs. [4–6]. The last one was realized by authors. However, the lack of reliable research in an aspect of photodetection properties of the common LEDs with regard to the bigger group is a serious barrier to develop such systems in the future. The article aims was addressing this issue.

Acknowledgement

The authors acknowledge the financial support from the Polish National Centre of Science under grant no 2011/03/B/ST7/00204.

References

- [1] E. Miyazaki, S. Itami, T. Araki, Using a light-emitting diode as a high speed, wavelength selective photodetector, *Rev. Sci. Instrum.* 69 (1998) 3751–3754.
- [2] Y.B. Acharya, Spectral and emission characteristics of LED and its application to LED-based sun-photometry, *Opt. Laser Technol.* 37 (2005) 55–550.
- [3] S. Bent, A. Moloney, G. Farrel, LEDs as both Optical Sources and Detectors in Bi-Directional Plastic Optical Fibre Links, *ISSC 2006*, Dublin Institute of Technology, 2006, pp. 345–349.
- [4] S. Schmid, G. Corbellini, S. Mangold, T.R. Gross, LED-to-LED Visible Light Communication Networks, *MobiHoc'13*, Bangalore, India, 2013, pp. 1–9.
- [5] H. Chun, S. Rajbhandari, G. Faulkner, D. Tsonev, H. Haas, D. O'Brien, Demonstration of a bi-directional visible light communication with an overall sum-rate of 110 Mb/s using LEDs as emitter and detector, *Proc. IEEE Photon. Conf. (IPC)* 132–133 (2014).
- [6] G. Stepniak, M. Kowalczyk, L. Maksymiuk, J. Siuzdak, Optical Wireless Transmission at Rates Beyond 100 Mbit/s Using LED both as Transmitter and Receiver, *IEEE Phot. Technol. Lett.* 27 (2015) 2067–2070.
- [7] M. Kowalczyk, J. Siuzdak, VLC link with LEDs used as both transmitters and photo-detectors, *Proc. of ICUFN'15* (2015) 893–897.
- [8] H. Miawarni, Basic VLC infrastructure design using two color diffuse LED as receiver and color intensity modulation, *J. Electron. Eng. Comp. Sci.* 1 (2016) 71–76.
- [9] L.T. Dung, S. Jo, B. An, Demonstration of low-complexity led-to-led two-way visible light communication system, *Proc. IEEE Symp. Compu. Consum. Control* 216–219 (2016).
- [10] Q. Wang, D. Giustiniano, D. Puccinelli, An open source research platform for embedded visible light networking, *IEEE Wireless Commun.* 22 (2015) 94–100.
- [11] S. Li, A. Pandharipande, F.M.J. Willems, Two-way visible light communication and illumination with LEDs, *IEEE Trans. Commun.* 99 (2016) 1.
- [12] F. De Santis, M. Ferrara, H-Ch. Neitzert, Optical in situ characterization of isotactic polypropylene crystallization using an led array in avalanche-photoreceiver mode, *IEEE Trans. Instrum. Measur.* 55 (2006) 123–127.
- [13] D.A. Bui, D. Anh, P.C. Hauser, Analytical devices based on light-emitting diodes—a review of the state-of-the-art, *Anal. Chim. Acta* 853 (2015) 46–58.
- [14] J. Rossiter, T. Mukai, A Novel Tactile Sensor Using a Matrix of LEDs Operating in Both Photoemitter and Photodetector Modes, in: *2005 IEEE Sensors*, Irvine, USA, 2005, pp. 994–997.
- [15] S. Li, F.M.J. Willems, Daylight sensing LED lighting system, *IEEE J. Sens.* 16 (2016) 3216–3223.
- [16] I.M.P. de Vargas-Sansalvador, C. Fay, et al., A new light emitting diode–light emitting diode portable carbon dioxide gas sensor based on an interchangeable membrane system for industrial applications, *Anal. Chim. Acta* 69 (2011) 216–222.
- [17] C. Weber, J.O. Tocho, E.J. Rodriguez, H.A. Acciaresi, LEDs used as spectral selective light detectors in remote sensing techniques, *J. Phys. Conf. Ser.* 274 (2011) 1–6.
- [18] S. Li, A. Pandharipande, LED-based color sensing and control, *IEEE J. Sens.* 15 (2015) 6116–6124.
- [19] S. Li, A. Pandharipande, F.M.J. Willems, Unidirectional visible light communication and illumination with LEDs, *IEEE Sens. J.* 16 (2016) 8617–8626.
- [20] D.Y. Shin, J.Y. Kim, I.Y. Eom, Spectral responses of light-emitting diodes as a photodiode and their applications in optical measurements, *Bull. Korean Chem. Soc.* 37 (2016) 2041–2046.
- [21] M. Kowalczyk, J. Siuzdak, Influence of reverse bias on the LEDs properties used as photo-detectors in VLC systems, *Proc. SPIE* 9662 (2015) 9662058–9662061.
- [22] S.O. Kasap, *Optoelectronics and Photonics*, 2nd edition, Pearson, 2012.
- [23] E.F. Schubert, *Light-Emitting Diodes*, 2nd edition, Cambridge University Press, Cambridge, 2014.
- [24] S. Nakamura, T. Mukai, Candelera-class high-brightness InGaN/AlGaIn double-heterostructure blue-light emitting diodes, *Appl. Phys. Lett.* 64 (1994) 1687–1689.
- [25] N.M. Haegel, S.E. Williams, C. Frenzen, C. Scandrett, Imaging charge transport and dislocation networks in ordered GaInP, *Physica B* 404 (2009) 4963–4966.
- [26] K. Kumakura, T. Makimoto, N. Kobayashi, T. Hashizume, T. Fukui, H. Hasegawa, Minority carrier diffusion length in GaN: dislocation density and doping concentration dependence, *Appl. Phys. Lett.* 86 (2005) 052105.
- [27] *Semiconductors and Semimetals*, 64, in: I. Electroluminescence, G. Mueller (Eds.), Academic Press, San Diego, 2000.
- [28] G. Schmiedel, P. Kiesel, G.H. Dohler, E. Greger, K.H. Gulden, H.P. Schweizer, M. Moser, Electroabsorption in ordered and disordered GaInP, *J. Appl. Phys.* 81 (1997) 1008–1010.